Real-time analysis for MBE by time-resolved core-level photoelectron spectroscopy

Fumihiko Maeda,[a]***†** **Yoshio Watanabe,**[a]**† Masaharu Oshima,**[a]**‡ Masami Taguchi**[b] **and Retsu Oiwa**[b]

[a]*NTT Science and Core-Technology Laboratory Group, Musashino-shi, Tokyo 180, Japan, and* [b]*ULVAC-PHI, Chigasaki-shi, Kanagawa 253, Japan. E-mail: fmaeda@will.brl.ntt.co.jp*

A system has been developed for the real-time analysis of surface reactions during molecular beam epitaxial growth which uses photoelectron spectroscopy with VUV light taken from synchrotron radiation. This system consists of a synchrotron radiation beamline and growth/analysis apparatus in which photoelectron spectroscopy is performed with sub-second time resolution. In this system, photoelectron spectra are measured in sequence by a 'non-scanning' measurement method that enables the acquisition of snapshot photoelectron spectra using a multi-channel detector. This non-scanning measurement method was enabled by equipping an electric field correction grid. This system was used to monitor the photoelectron spectra of a GaSb(001) surface.

Keywords: real-time analysis; crystal growth; surfaces; core levels; time-resolved photoelectron spectroscopy.

1. Introduction

To clarify the process of molecular beam epitaxy (MBE) growth, various techniques which analyse growing surfaces have been developed. These techniques require sub-second time resolution to detect the changes occurring on growth surfaces during several-second periods of MBE growth, which we call 'real-time' analysis methods. Moreover, the techniques need a surface sensitivity of a few monolayers. Reflection high-energy electron diffraction (RHEED) is one of the most popular and well established methods because the RHEED apparatus is part of most MBE growth systems. This method can provide surface structural information. Several real-time analysis techniques using diffraction, such as grazing-incidence X-ray diffraction (GIXD), can also provide surface structural information.

However, these methods cannot analyse surface bonding states, which provide chemical reaction information. Therefore, few attempts have been made to obtain surface chemical information. Reflection difference (RD) and surface photoabsorption (SPA), which detect dielectric response, are two such methods. These methods are powerful tools for analysing systems, such as GaAs growth, which have been well investigated. However, RD and SPA have not been applied to other hardly investigated

systems as chemical analysis tools because these methods require complex theoretical analysis.

Hence, we have developed a novel real-time analysis system which uses core-level photoelectron spectroscopy (PES) excited by vacuum-ultraviolet light (VUV) from synchrotron radiation. Core-level PES is often called electron spectroscopy for chemical analysis (ESCA); it is one of the most suitable methods for chemical bonding analysis. Furthermore, by using an appropriate energy VUV from synchrotron radiation for excitation, the probed depth can be limited to a few monolayers from the surface and the photoelectron intensity is strong enough for real-time analysis. However, using conventional photoelectron measuring systems, time resolution is, so far, at least several seconds. Therefore, in the photoelectron measurement of this system we try to use a 'non-scanning' electron measurement method in which a multi-channel detector (MCD) obtains the photoelectron spectrum by utilizing only the energy dispersion of this MCD. This measurement is key to achieving sub-second acquisition of the core-level photoelectron spectrum. In this paper a real-time analysis system and a modification of the photoelectron measurement system to achieve the non-scanning measurement are described. Then, time-resolved core-level PES results with sub-second time resolution on GaSb(001) are presented to demonstrate its effectiveness.

2. Real-time analysis apparatus

Fig. 1 is a schematic view of the analysis apparatus (Maeda *et al.*, 1996). It consists of a sample introduction chamber (I), a sample preparation chamber (II), a real-time growth analysis chamber (III), a chamber for changing the sample transfer direction (IV), and a conventional MBE growth chamber (V). The MBE chamber (V) allows buffer layers to be grown to provide a clean flat surface for real-time analysis. In the real-time growth analysis chamber (III), crystal growth and photoelectron spectroscopy are performed simultaneously. It thus contains a photoelectron analyser (shown as 1) and up to three effusion cells (2). This photoelectron analyser is based on the PHI ESCA 5400 system, which includes a hemispherical electron analyser and an electrostatic field lens. A conflat flange (3) is used as a port for the synchrotron radiation beamline. A sample manipulator (4) is installed from the top of the chamber at an angle of 20° to the vertical. In addition to these main parts for real-time growth analysis by photoelectron spectroscopy, there is a mono-
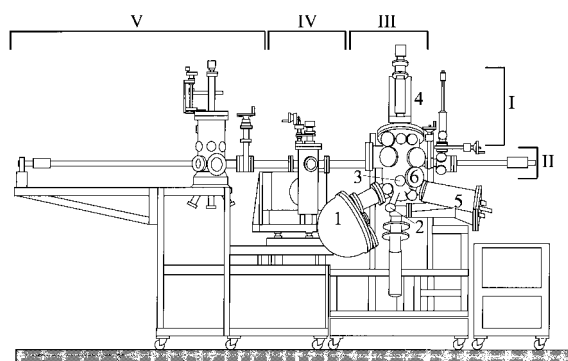

Figure 1
Side view of real-time growth/analysis apparatus. See text for explanation of numbers.

chromated X-ray source (5) and RHEED apparatus (6) (only the screen is shown in Fig. 1).

To obtain a core-level photoelectron spectrum with sub-second acquisition time we used a 'non-scanning' measurement technique which enables the acquisition of snapshot photoelectron spectra without the need for kinetic energy scanning with an electrostatic lens. For kinetic energy scanning, the electric voltage supply to the electrostatic lens of the electron analyser should be reset. Hence, wait time should be introduced after the voltage resetting. As a result, the acquisition time cannot be reduced to less than several seconds by the conventional 'scanning' measurement method. Therefore, the non-scanning method greatly decreases the spectrum acquisition time because the electrostatic field does not have to be reset and all detected electrons are used in the spectrum. However, the non-scanning measurement is not usually used because electrons cannot be detected uniformly by the different channels of an MCD, the result being that the measured spectrum is strongly influenced by the sensitivity of each channel in the MCD. Therefore, to enable non-scanning measurement, the conventional photoelectron measurement system was modified.

First, an MCD whose electron detection efficiency has very low positional dependence was installed. Then, we found that the electrostatic field correction between the hemisphere of the electron analyser and the MCD was also important. We therefore examined the best shape of the grid for electrostatic field correction. The three grids examining the field correction effect are shown on the right-hand side of Fig. 2. As an experiment, one of these grids was put in front of the MCD surface, where photoelectrons strike after being emitted from the exit between the inner and outer spheres of the electron analyser. Next, photoelectron spectra, which are almost constant intensities, were measured. The excitation source was Al $K\alpha$ and the centre binding energy for photoelectron detection was set at 1420 eV, at which secondary electrons with no spectrum structure can be detected with high intensity.

When the path energies (E_p) of the electron analyser were set at 16.7 and 83.4 eV, the spectra were obtained by using three grids, (a), (b) and (c), as shown in Fig. 2. When grid (a) was used, both resulting spectra do not show a symmetric constant pattern, but show a pattern in which the intensity decreases with increasing kinetic energy. Furthermore, the intensities decrease
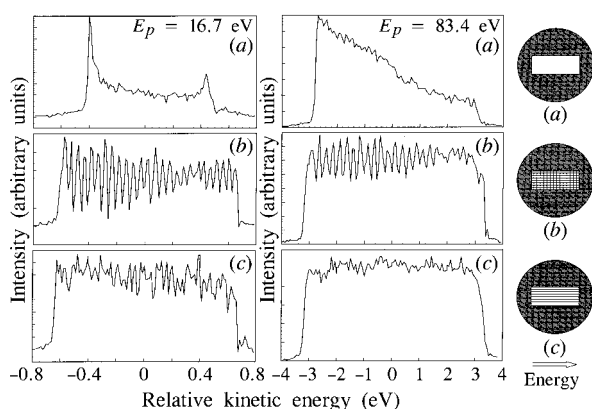
remarkably at both sides, with widths of 0.3 eV for the 83.4 eV spectrum and 0.2 eV for the 16.7 eV spectrum, compared with the intensities in (b) and (c). For grids (b) and (c), the envelopes, which show almost constant intensity within a detection window, are almost the same in both path energy spectra. Grid (b), however, shows periodic zigzag changes in intensity. The number of zigzag peaks and troughs equals the number of Au strip wires along the vertical to the innersphere–outersphere direction. Basically, each characteristic appears to be the same for the two path energies, although the intensities are weaker and the characteristics are more emphasized in the 16.7 eV case than in the 83.4 eV case.

These results show that the spectrum intensity modulation was induced because of electric field distortion at the grid edge. Hence, in case (a), where no grid is covered within the detection area, this edge effect, which is caused by both sides of the detection window, appears directly. However, in grid (b), the effect caused by both sides is weaker and the strips of Au wire act as edges and the edge effect is induced by these strip wires. Therefore, we can conclude that grid (c) is the best shape for electric field correction. In this case we believe that the edge effect appears between the strip wires along the innersphere–outersphere direction. This, however, does not appear in the energy spectrum because the direction is vertical to the direction of the energy.

3. Performance

The experiments using this apparatus were performed (Maeda *et al.*, 1997) at ABL-3B, which is installed at the normal-conducting accelerating ring at NTT SOR in Atsugi, to show the feasibility of real-time analysis by time-resolved core-level photoelectron spectroscopy. Sb desorption from GaSb(001) was chosen for the preliminary experiment. The samples were prepared by growing a 20 nm-thick buffer layer and showed a clear c(2 × 6) RHEED pattern at room temperature. Then, these samples were annealed to 793 K and the Sb supply was controlled during photoelectron measurements. The photoelectron spectra of Ga 3d and Sb 4d were measured at intervals of 0.5 s. For these measurements the photon energy was set at 90 eV and the path energy of the
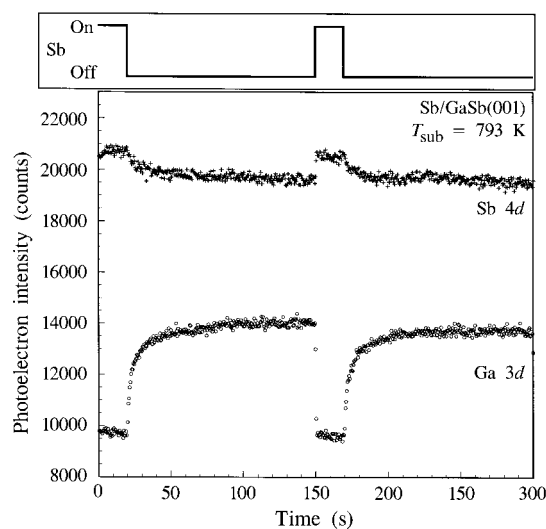

Figure 2
Secondary electron spectra recorded by a non-scanning measurement method. (a), (b) and (c) correspond to the electric field correction grid shapes illustrated on the right-hand side. Grid (a) has a rectangular through window. Grids (b) and (c) were altered from grid (a) by adding a mesh and strips of Au wire, respectively.

Figure 3
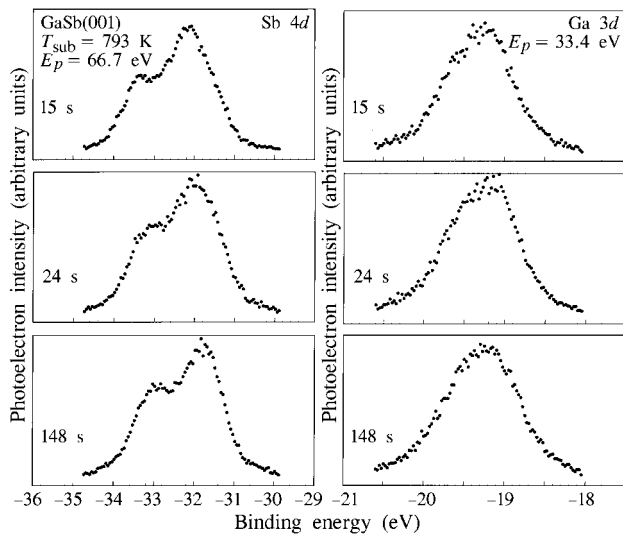Time dependence of Ga 3d and Sb 4d photoelectron intensities.

Figure 4
Sb 4*d* and Ga 3*d* photoelectron spectra under Sb flux and during Sb desorption.

electron analyser was set at 33.4 eV for Ga 3*d* and 66.7 eV for Sb 4*d*.

First, before this experiment, the limit on the time resolution of this system was experimentally obtained by measuring the time for taking the Ga 3*d* spectrum. When we set the data recording time to 50 ms, which is the net time for detecting photoelectrons in the MCD, it took 65 s to obtain 600 spectra (not shown here). This means we measured one spectrum every 109 ms. Therefore, this real-time analysis system takes at least 60 ms per spectrum

when the spectra are measured continuously, with most of the time being spent transferring data from the MCD to the controlling computer, displaying the data on the display and storing the data on disk. Therefore, 60 ms is the limit of this system at present. However, this result shows that this system could measure one photoelectron spectrum every 0.1 s.

Next, as shown in Fig. 3, we obtained the time dependence of Ga 3*d* photoelectron intensities. In this figure, at a time of 150 s, the changes occurred in about 1 s and can be traced by both Ga 3*d* and Sb 4*d* intensities, indicating that this figure reflects the surface composition changes with a sub-second time resolution. Fig. 4 shows photoelectron spectra corresponding to the data points in Fig. 3. The spectra in Fig. 4 are the sum results of three spectra, at 0.5 s, 0.5 s before and 0.5 s after the time shown on the left-hand side of each spectrum. In the spectra, the influences of the detection characteristics are almost negligible and the shape changes in the spectra responsible for surface bonding structures can be detected. These results show the possibility of site-specific analysis of MBE growth by time-resolved core-level photoelectron spectroscopy using our apparatus.

References

Maeda, F., Watanabe, Y., Muramatsu, Y. & Oshima, M. (1996). *Jpn. J. Appl. Phys.* pp. 4457–4462.
Maeda, F., Watanabe, Y. & Oshima, M. (1997). *Phys. Rev. Lett.* **78**, 4233–4236.